NEW HIGH-TEMPERATURE MATERIALS AND METHODS OF INVESTIGATING THEIR THERMOPHYSICAL PROPERTIES AT TEMPERATURES UP TO 3500° C

V. I. Tyukaev and A. G. Shashkov

Inzhenerno-Fizicheskii Zhurnal, Vol. 12, No. 2, pp. 263–277, 1967

UDC 536.2.08

I. HIGH-TEMPERATURE MATERIALS

New technology involves increases in all the various process parameters: temperature, velocity, pressure. Accordingly, it calls for new materials with much improved properties—resistance to heat and corrosion, fusibility, semiconducting properties, lightness, hardness—for use in solving such problems as the conversion of various forms of energy into electricity (MHD generators, atomic power stations, thermionic converters, solar energy devices, fuel cells) and the design of high-speed aircraft [1].

One of the most important problems currently engaging the attention of materials scientists in various countries is the development and investigation of new refractories.

Our aim has been to review the most promising high-temperature materials, their specific applications and methods of investigating their thermophysical properties at temperatures up to 3500° C.

Refractory compounds may be classified as follows:

1. Compounds of transition metals and nonmetals—borides, carbides, nitrides, oxides, silicides, phosphides, and sulfides.

2. Compounds of nonmetals—carbides, nitrides, and sulfides and phosphides of boron and silicon together with boron-silicon alloys.

3. Compounds of metals—intermetallides.

Compounds of the first class have an internal and external similarity with metals and intermetallides; therefore they may be called metalline. Since the metallic components are transition elements, the chemical bond involves the s and p electrons of both components and the additional d and *f* levels of the metal. The stability of the electron shells determines the refractoriness. The predominance of metallic or nonmetallic properties is determined by the relationship between the acceptor activity of the metal atoms and the ionization potential of the nonmetal. For example, in compounds involving a nonmetal with a low ionization potential (silicon) and an inactive metal (molybdenum) semiconducting properties predominate. But if we take a nonmetal with a high ionization potential (carbon), then with the same metal we obtain a metalline compound, i.e., predominance of metallic and ionic bonds gives metallic and nonmetallic properties, respectively.

Compounds of the second class also have bonds of two kinds, but with a covalent bond of the B-B type predominating, which leads to semiconducting properties and high electrical resistance at room temperature. As a rule they decompose before the melting point or melt with decomposition.

Compounds of the third class form the subject matter of the recently created science of metal chemistry.

The above classification was proposed by G. V. Samsonov. *

Further acquaintance with refractory (high-melting) compounds reveals that 125 of them have a melting point above 2000° C and 16 above or equal to 3000° C. These figures do not include refractory metal oxides and pure high-melting metals. Naturally, the characteristics of the top 16 compounds are of most immediate interest. Table 1 gives the properties and applications of some high-melting materials. With respect to the rest our choice has been based on the usefulness of their properties and their applications in modern technology.

MATERIALS USED IN REACTOR CONSTRUCTION

In making the fuel elements for fast-neutron reactors with liquid-metal cooling it is necessary to employ metals with a small fast-neutron capture cross section that are both cheap and easy to work. Their properties are presented in Table 2. The data of this table were taken from Turner's report "Manufacture of Fuel Elements for Fast-Neutron Reactors at Downtree" (Proceedings of the Second International Conference on the Peaceful Uses of Atomic Energy, 1958).

Niobium may be used for the outer jacket and vanadium for the inner jacket, which under emergency conditions makes it possible to withdraw the molten fuel from the danger zone together with the coolant through the destroyed vanadium jacket.

The trend toward an increase in reactor temperature has made it necessary to use ceramic nuclear fuels. The matrix elements for dispersed UO_2 fuels are the oxides Al_2O_3, BeO, MgO, ZrO_2 and ThO_2, which have a low neutron-capture cross section and high melting points. USi_2 and USi_3 disperse fuels require a $MoSi_2$ matrix since the latter possesses high resistance to oxidation and a high melting point. The matrices protect the uranium silicides by enveloping them.

It has recently been suggested that the efficiency of atomic power stations could be improved by adding a loop with a MHD generator. However, for the latter to operate normally, the temperatures at the inlet should be not less than 2200°–2750° C, i.e., the working gas cooling the reactor is heated to that tempera-

*G. V. Samsonov, in: High-Temperature Metal-Ceramic Materials [in Russian], Kiev, 1962, p. 11.

Table 1

Properties and Applications of the Top High-Melting Compounds

No.	Chem. symbol	t_m, °C	Thermal conductivity			Specific heat			Properties and applications
			t, °C	accuracy, %	reference	t, °C	accuracy, %	reference	
1	TiB_2	2980	1500	—	[2, 3]	2300	1,2	[4]	Resists neutron radiation [5]. Thermoelectrodes
2	ZrB_2	3040	200	—	[6]	800	—	[7]	Heat-resistant
3	NbB_2	3000	200	—	[6]				Heat-resistant
4	TaB_2	3100	200	—	[8]				Heat-resistant
5	TiC	3147	2100	5	[9]	1500	1	[10]	Resists molten metals. Heat shielding [11]
6	ZrC	3530	2700	25	[12]				Scale-resistant, low neutron-capture cross section
7	NbC	3480	2400	20	[12]	1530	—	[13]	Resistant to metal vapors. Very hard
8	TaC	3880				1800	—	[14]	Cutting tools [15], crucibles [16], heaters [17], electric lamps [18]
9	TiN	3205	950	—	[19]	1550	1	[10]	Heat-resistant, hard
10	ZrN	2980	800	—	[19]	1550	2	[20]	High electrical conductivity
11	TaN	3087	20	—	[17]	527	4	[20]	

Table 2

Materials for Fuel-Element Cans

Element	Atomic weight	γ, g/cm^3	t_m, °C	$Q_{f.n}$, barns	Workability
Ti	47.90	4.5	1725	79	Good
Zr	91.22	6.5	1860	43	Good
Hf	178.6	—	1876	—	Good
Nb	92.91	8.57	2460	92	Very good
Ta	180.88	16.6	3000	250	Good
Mo	95.95	10.2	2620	68	Not bad
W	183.92	19.3	3410	117	Poor
Re	186.31	20.0	3170	—	Poor
V	50.95	6.02	1900	10	Good
Ni	58.69	8.9	1455	40	Good

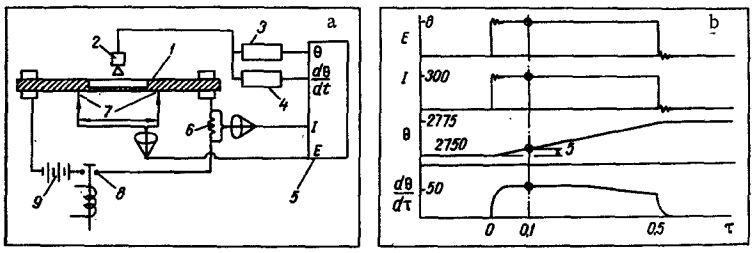

Fig. 1. Measuring system for determining specific heats to 3600° C (1 is the specimen, 2 is the photoelectric pyrometer, 3 is the potentiometer, 4 is the differentiator, 5 is the oscillograph, 6 is the current shunt, 7 are the potential probes, 8 is the relay, 9 are the storage batteries) (a) and oscillograms of voltage, current, temperature, and heating rate (b) (E in volts, I in amps, θ in °C, τ in sec).

ture. If seeding with alkali-metal salts proves possible, the working temperature of the gas in the system could be much reduced.

The working temperature of solid-fuel reactors is determined by the maximum fuel element temperature. In the Los Alamos experimental reactor, working on a solid solution of uranium carbide and zirconium carbide, it was 2200° C. Of course, the nuclear fuel was uranium, and the other components were used only on account of the high heat resistance and low neutron-capture cross section.

The limitation on working temperature is removed in reactors working with gaseous fissionable material since the temperature of the latter may be twice as high as the temperature of the walls. The fissionable gas is either itself the working medium of the MHD generator or enters into its composition. The maximum gas temperature is of the order of 5500° C.

The working channel of a MHD generator requires a high-melting erosion-resistant material, possibly a metal carbide. However, in a combined system the material must also be able to withstand gamma radiation and neutron bombardment.

Another method of direct conversion of nuclear energy into electricity is thermionic conversion in plasma diodes built into the fuel elements. So far, tungsten and tantalum have generally been used as cathode materials. Research is now being concentrated on such heat-resistant materials as metal nitrides and carbides, which are capable of working inside reactors for long periods at temperatures of the order of 2200° C.

The above methods of converting nuclear energy into electricity are impracticable unless the problem of developing and investigating heat-resistant materials can be solved. However, solution of this problem will make possible the construction in the near future of plants with an over-all efficiency of the order of 60% as compared with 40% for the best contemporary power stations.

MATERIALS USED IN ROCKET ENGINEERING

The working conditions in rockets are such as to require high heat-resistance, high resistance to thermal shock, and resistance to scaling at temperatures above 1300° C.

The following materials are employed to protect nose cones, thrust chamber walls, and other components:

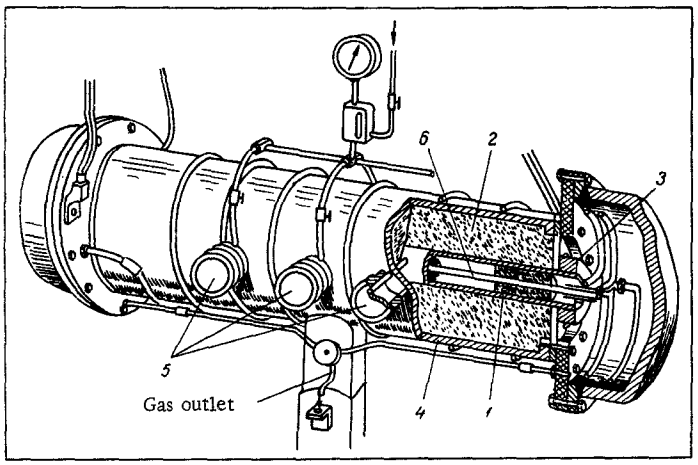

Fig. 2. Sketch of graphite tube furnace for determining specific heats to 3600° C: 1) graphite heater tube, 2) thermal insulation, 3) electrode, 4) furnace shell, 5) sight tubes, 6) specimen.

1. Light metals and their alloys, e.g., titanium. Beryllium has been used as heat shielding for a manned spacecraft [21,22].

2. High-melting metals, niobium, molybdenum, and their alloys. These all have a serious and not easily eliminated shortcoming—their ease of being oxidized [23,24,25].

3. Cermets, metals impregnated with solid components, e.g., borides, carbides, nitrides [24].

4. Ceramic materials—oxides of aluminum, magnesium, thorium, together with chlorides, fluorides and hard alloys used for heat shielding [24].

5. Graphite whose strength at the sublimation point is higher than its strength at room temperature. Its greatest disadvantage is oxidizability. Remarkable properties are possessed by pyrolytic anisotropic graphite. By using it as a heat conductor it has proved possible to make a perfectly reliable throat section for the supersonic nozzle of a solid-propellant rocket motor. The permissible temperature was 2800° C, the decomposition temperature, 3650° C. With respect to warmup rate for the entire mass of the throat liner pyrographite was twice as effective as tungsten [26].

6. Plastics based on various resins that liberate large quantities of gas in the course of degradation [24].

In view of the specific conditions of rocket operation, e.g., short burns and aerodynamic heating, composite materials are of special interest. A study of homogeneous high-temperature materials has shown that they do not possess all the necessary properties. The desired properties cannot be obtained by introducing admixtures. In composite materials each component or layer performs its own function.

For ablative heat shields it is customary to use organic coatings (epoxy and polyurethane resins) and ceramic oxides impregnated with organic compounds.

Composite materials are especially valuable for the nozzles of rocket motors with thrust chamber temperatures of the order of 3900° C. Tungsten and graphite are no longer suitable. Nozzles for solid-propellant rocket motors have recently been made of porous tungsten impregnated with another metal with a lower melting point and a boiling point lower than the nozzle working temperature. In this case protection is provided by the heat capacity of the system as a whole and the phase transitions of the low-temperature metal [27].

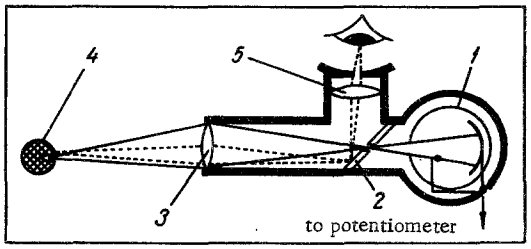

Fig. 3. Diagram of photoelectric pyrometer: 1) phototube, 2) mirror with central hole, 3) objective lens, 4) specimen, 5) ocular lens.

II. METHODS OF INVESTIGATING THE THERMOPHYSICAL PROPERTIES OF HIGH-TEMPERATURE MATERIALS

METHODS OF DETERMINING SPECIFIC HEAT

There are nonstationary and stationary methods of determining specific heat. The former has the advantage that it enables the temperature dependence of the true specific heat to be determined directly. We will consider two variants.

Rasor and McClelland [28] have determined the specific heat of electrical conductors in the range 1000°–3600° C by the direct heating method. This method is illustrated in Fig. 1.

The specimen was heated to the required temperature in a graphite tube furnace (Fig. 2) after which a constant current was passed through it. The heating rate was 50 deg/sec. In the region close to the axis of the specimen the temperature increases linearly for 0.1 sec, i.e., by 5° C. The specific heat is calculated from the expression

$$c_p = EI/m\,(dT/d\tau). \qquad (1)$$

The absolute temperature of the specimen was determined with an optical pyrometer, while exact measurement of the 5° temperature change was made possible by the specially designed photoelectric pyrometer shown in Fig. 3. After special calibration the

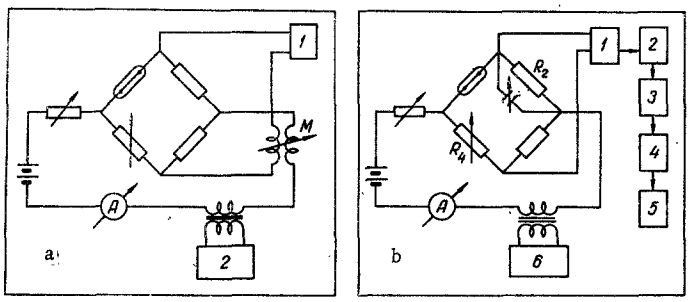

Fig. 4. Circuit diagrams of devices for determining specific heats to 3300° C: a) using mutual inductance (1, selective amplifier, 2, low-frequency oscillator) and b) using capacitance with block diagram of indicator system (1, selective amplifier, 2 and 4, phase shifters, 3 and 5, synchronous detectors, 6, audio oscillator).

rate of change of specimen temperature can be determined as

$$\frac{dT}{d\tau} = \frac{T^2 d\theta}{b\theta d\tau}. \quad (2)$$

The error in determining the specific heat was ±5% and depended mainly on the error in determining the parameter b of the photocell.

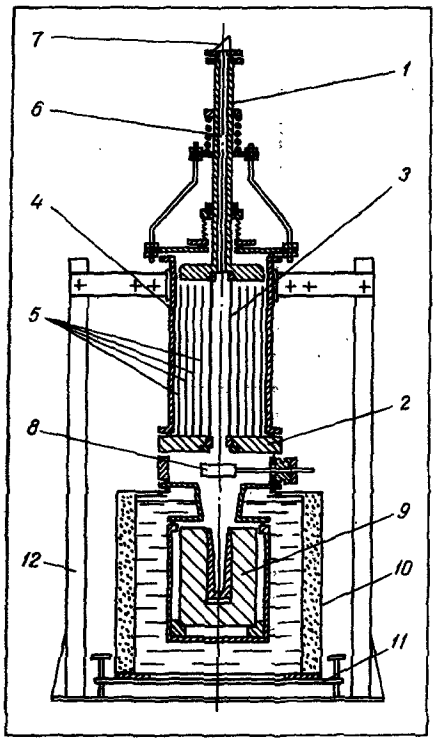

Fig. 5. Diagram of apparatus for determining enthalpy and specific heat to 2500° C: 1 and 2) upper and lower cooled conductors, 3) tungsten heater, 4) cooled furnace shell, 5) screens, 6) optical channel, 7) total internal reflection prism, 8) cooled screen, 9) calorimeter, 10) thermostatted jacket, 11) carriage, 12) stand.

This method was used to determine the specific heat of graphite, various carbides, and for samples of high-temperature metals protected by a tantalum tube.

Ya. A. Kraftmakher [29] has developed a modulation method of measuring the specific heat of high-melting metals up to the melting point based on the laws of the regular thermal regime of the third kind. If a current $I = i_0 + i \sin \omega\tau$ ($i \ll i_0$), flows through the specimen, its temperature and resistance vary according to a periodic law

$$T = T_0 + \theta, \quad \Delta R = R_0 \alpha\theta.$$

The power balance of the specimen is given by the expression

$$mc\frac{d\theta}{d\tau} + f(T_0) + \left[\frac{df}{dT}\right]_{T_0}\theta = i_0^2 R + 2i_0 i R \sin\omega\tau + i_0^2 R_0 \alpha\theta. \quad (3)$$

After the substitution $f(T_0) = i_0^2 R$, the solution of differential equation (3) is obtained in the form

$$\theta = \theta_0 \sin(\omega\tau - \varphi), \quad (4)$$

where

$$\theta_0 = \frac{2i_0 iR}{mc\omega}\sin\varphi, \quad \operatorname{tg}\varphi = \frac{mc\omega}{K}, \quad K = \left[\frac{df}{dT}\right]_{T_0} - i_0^2 R_0 \alpha.$$

We can now find the specific heat from the expression

$$mc = \frac{2i_0 iR}{\omega\theta_0}\sin\varphi. \quad (5)$$

Thus, the specific heat depends only on the ratio of the amplitudes of the current and temperature oscillations, which makes it possible to design compensation measuring circuits (Fig. 4). In the case of a circuit using mutual inductance the expression for the specific reduces to the form

$$mc = 2i_0^2 RR_0 \alpha/\omega^2 M. \quad (6)$$

In the case of a circuit using capacitance the expression for the specific heat becomes

$$mc = \frac{2i_0^2 R_0 \alpha}{\omega^2 RC}\sin^2\varphi. \quad (7)$$

When the specimens took the form of wires 0.03–0.05 mm in diameter, the modulation frequency was about 120 Hz. The experiments were performed in an argon atmosphere and under vacuum. The temperature of the specimens was determined from electrical resistance. The scatter of the experimental values was about 1% up to temperatures of 3300° K, increasing to 4% at 3600° K. Unfortunately, the accuracy was not computed.

Among the stationary methods of determining specific heat at very high temperatures the one giving the most accurate results is the mixing method using a massive calorimeter and diathermal heat measurement. An experimental apparatus based on this principle has been developed by Kirillin, Sheindlin, and Chekhovskii [30–32] (Fig. 5). It consists of a high-temperature furnace and a massive copper calorimeter separated by a screen system to prevent furnace radiation entering the calorimeter during heating of the sample and calorimetry. The furnace and the calorimeter are evacuated to a pressure of 10^{-3} mm Hg. The experiment is conducted in a vacuum or in a protective argon atmosphere at 770 mm Hg.

The calorimeter was calibrated by heating with electric current, while in analyzing the results of the experiments values of the temperature determined with the platinum resistance thermometer were excluded. For a known calorimeter heat value the heat effect is given by

$$Q = A\Delta t = (Q/\Delta t)_{\text{calib}}\,\Delta t. \quad (8)$$

Since during calibration and in the experiments the initial temperature of the main period was equal to

22° C (for convenience), the values of Δt in the numerator and denominator of Eq. (8) are the same, i.e., for a linear temperature-resistance relation Q can be uniquely determined in terms of ΔR.

Generally speaking, a platinum resistance thermometer has a parabolic temperature-resistance characteristic. However, at room temperature it is quite possible to replace it with a linear characteristic if the temperature difference $\Delta t \leq 10°$ C [32]. This substitution increases the accuracy and partly eliminates the need to calibrate the resistance thermometer.

As a result of calibration of the calorimeter we obtained the relation

$$(Q/\Delta R)_{\text{calib}} = f(\Delta R). \quad (9)$$

The corrections for heat transfer were mainly 2–3%. The temperature of the sample in the furnace was measured up to 1300° C with second-class platinorhodium/platinum reference thermocouples, and above that temperature with OP-48 and Pyrolux-II optical pyrometers.

Various materials have been investigated by this method.

The enthalpy is calculated from the formula

$$i^{t_a}_{0°C} = \frac{1}{G}(A\Delta R + q_f - q_w) + i^{t'_n}_{0°C}. \quad (10)$$

The corrections q_f and q_w were calculated theoretically. The maximum relative error of the experimentally determined enthalpy and mean specific heat at temperatures of 2500° C was ±1.2%.

After the heater had been redesigned, it proved possible to reach temperatures of 2800° C [33], and, using a graphite heater, even 3100° C [34]. A temperature of 3500° C can be obtained at a pressure in the apparatus of the order of 10 bar.

To sum up the methods described above, it may be said that at temperatures up to 3500° C the nonstationary methods can be used only to determine the specific heat of electrical conductors correct to 5%, while the mixing method is suitable for determining the mean specific heat of various solids and liquids (in ampuls) up to temperatures of 3500° C with an accuracy of up to 2%.

METHODS OF DETERMINING THERMAL CONDUCTIVITY

Rasor and McClelland [28] have developed an apparatus (Fig. 6) for determining thermal conductivity up to 2700° C based on the external heating method. The specimens are placed in a graphite furnace working on dc. In order to obtain temperature uniformity along the length of the hollow cylindrical specimen, the power of the protective end-face heaters ("yokes") can be independently regulated by means of individual transformers. The radial heat flow through the specimen is recorded by means of a water-cooled heat sink located axially inside the specimen. The temperature distribution along the axis of the sample and the radial temperature drop are determined with an optical pyrometer through special sight holes.

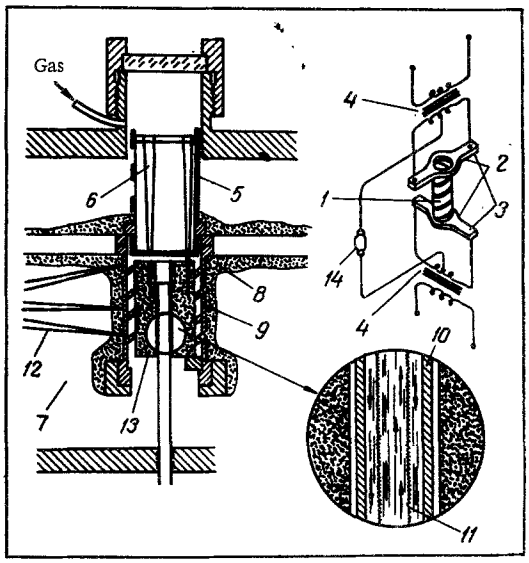

Fig. 6. Diagram of apparatus for determining thermal conductivity to 2700° C: 1) heater, 2) graphite "yokes," 3) soldering points for copper conductors, 4) regulating transformers, 5) thermal end insulation, 6 and 12) sight holes, 7) carbon black, 8) carbon wool, 9) helical graphite heater, 10) outer tube of heat sink (stainless steel), 11) glass tube, 13) specimen, 14) dc generator.

The thermal conductivity is calculated from the formula

$$\lambda = q \ln(r_2/r_1)/2\pi l \Delta t. \quad (11)$$

Metal specimens are protected from carbon vapor by means of a tantalum tube. Higher temperatures cannot be obtained on this apparatus owing to the necessity for a sharp increase in heater current.

The accuracy of this method is estimated at 5%.

At temperatures above 2700° C Rasor and McClelland determined the thermal conductivity of conducting materials by the direct heating method on the same graphite tube furnace as they used to determine specific heat (Fig. 2). The power supplied to the working section was dissipated from the surface; therefore the thermal conductivity could be found from the formula

$$\lambda = I^2 R/4\pi^2 r^2 \Delta t. \quad (12)$$

The electrical resistance is calculated from experimental data on the specific heat. The temperature difference is determined with an optical pyrometer.

The accuracy of the method is estimated at 8%.

Timrot and Peletskii [35] used electronic heating to investigate the thermal conductivity of high-melting metals and their alloys.

A specimen of diameter D and length L is suspended in a vacuum chamber. One end of the specimen

is supplied with a stationary heat flux Q_0 to create a certain temperature distribution T(x, r). For known values of the specific radiative losses $q_s(T)$, assuming a one-dimensional temperature field in the specimen, the thermal conductivity may be found from the expression

$$\lambda = \left(\pi D \int_x^L q_s(x)\,dx + q_{s2}\frac{\pi D^2}{4}\right) \Big/ \left.\frac{\pi D^2}{4}\frac{dT}{dx}\right|_x . \quad (13)$$

The circuit diagram of the apparatus is shown in Fig. 7. The operating conditions—vacuum of $5 \cdot 10^{-5}$ mm Hg, anode voltage 5–10 kV—make it possible to

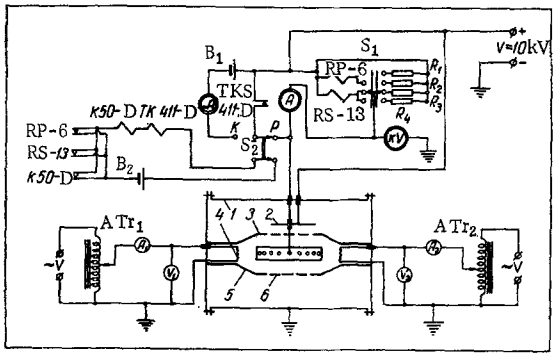

Fig. 7. Circuit diagram of apparatus for determining thermal conductivity up to 2300° C: 1) housing of apparatus, 2) screen, 3) specimen, 4) cathode, 5) focusing system, 6) suppressor grid.

neglect the secondary electron work function and the energy losses due to ionization of the residual gases in the heat flow calculations. The specific radiative losses are determined on a very short specimen (L/D = = 0.2–0.5) and are referred to the mean temperature of the specimen. In the experiments an optical pyrometer was used to determine the temperature distribution along the length of the specimen and the electronic heat flux, as the product of the accelerating voltage U and the emission current I.

The maximum relative error in determining the thermal conductivity at temperatures up to 2600° K is of the order of 15%. After making certain improvements in the apparatus and method Voskresenskii [36] succeeded in reducing the error to 10%.

METHODS OF DETERMINING THERMAL DIFFUSIVITY

The continuous heating method with variable heating rate is applicable whenever the temperature variation is monotonic and smooth and makes it possible to obtain the temperature dependence of the thermal diffusivity in one experiment [37, 38].

With account for the temperature dependence of the thermophysical properties the differential equation of heat conduction for an infinite solid cylinder may be written in the form

$$\rho(t)c_p(t)\frac{\partial t}{\partial \tau} = \lambda(t)\left(\frac{\partial^2 t}{\partial r^2} + \frac{1}{r}\frac{\partial t}{\partial r}\right) + \frac{\partial \lambda(t)}{\partial r}\frac{\partial t}{\partial r}. \quad (14)$$

The general solution of this equation is an infinite series, but in the principal stage of the heat conduction process it is possible to confine oneself to two terms. After the temperature difference between two points of the specimen has been determined experimentally the thermal diffusivity can be found from the following expression:

$$a = \frac{R^2}{4\Delta t}\frac{d}{d\tau}\left(t_0 + \frac{1}{4}\Delta t\right)(1-\eta),$$

$$\eta = \frac{1}{4a}\frac{da}{dt}\Delta t. \quad (15)$$

Expressing the temperature lag on the axis as $\Delta t = (dt_0/d\tau)\Delta\tau$, we obtain the other formula

$$a = \frac{R^2}{4\Delta\tau}(1+\varepsilon+\eta), \quad (16)$$

where $\varepsilon = -(1/4\Delta t)(d\Delta t/d\tau)\Delta\tau$ takes into account the nonconstancy of the heating rate. If $\varepsilon = \eta = 0$, the quasi-stationary heating regime is obtained. Owing to the finite size of the specimen the temperature distribution along its length is nonuniform, which can be taken into account by introducing the correction

$$\beta = \frac{1}{2}\left(\frac{d}{l}\right)\frac{\Delta t_l}{\Delta t}.$$

Generally speaking, the time lag may depend on the conditions of heat exchange with the ambient medium. However, it turns out that if one takes a point at which the temperature is equal to the mean temperature over the section and a point on the axis, then the time lag is almost independent of the heat transfer conditions at the surface of the specimen. In [39] it was found that for a cylinder the coordinate of this point x = 0.707R.

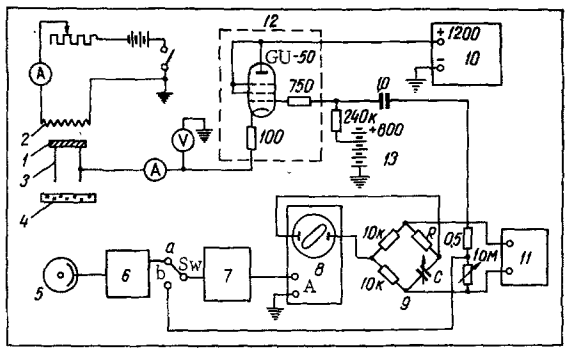

Fig. 8. Electrical diagram of apparatus for determining thermal diffusivity to 3000° C: 1) specimen, 2) cathode, 3) support, 4) absorbing wedge, 5) photocell, 6) cathode follower, 7) selective amplifier, 8) oscillograph, 9) phase shifter, 10) power source, 11) audio oscillator, 12) modulator, 13) regulated voltage source.

Thus, to determine a for any type of boundary and heat transfer conditions it is sufficient to measure the temperature difference between two points or the corresponding time lag. The method is evidently applicable at temperatures above 1000° C [40].

The method of the regular regime of the third kind has been used by Kraev and Stel'makh [41] to determine the thermal diffusivity of tungsten in the range 1600°–3000° C. A schematic of the experimental apparatus is shown in Fig. 8. The specimen in the form of a plate, is heated by a stream of electrons accelerated in a vacuum by a voltage $U = U_0 + \Delta U \cos \omega\tau$, where $\Delta U < U_0$. On the back of the plate a temperature phase lag develops. At temperatures up to 3000° C under vacuum conditions for a plate 0.1–0.5 mm thick Bi ~ 0.001–0.01. At $z = (Pd)^{1/2} > 2$ the phase shift is almost independent of Bi and can be determined from the phase shift at the phase shifter using the formula

$$\operatorname{tg} \frac{\varphi}{2} = \omega RC. \tag{17}$$

The value of z is found from the relation $\varphi = f(z)$, and the thermal diffusivity is calculated from the expression

$$a = \omega\delta^2/z^2. \tag{18}$$

The temperature of the specimens was determined with a OPPIR-017 optical pyrometer. The maximum error in determining the thermal diffusivity was 5%.

CALCULATION OF ABLATIVE MATERIALS

Since we are considering methods of investigating solids at very high temperatures, it is also worth mentioning a method of calculating ablative materials.

In the case of charring plastic the heat shield is (in section) a laminated system consisting of the charred layer, the reaction zone, and the unaffected plastic. The various gases formed in the reaction zone are sucked through the porous charred layer to the surface of the material. Having constructed the differential conservation equations for each chemical substance individually, we can solve them on a computer if we know the decomposition reaction kinetics and the thermal and mechanical characteristics of the charred layer. As for the thermophysical properties of the charred layer—specific heat, thermal conductivity, and thermal diffusivity—they can be fully investigated by the methods of high-temperature thermophysics described above.

In [42], on the basis of theoretical calculations of the mechanical and temperature stresses caused by the pressure and temperature gradients in the charred layer, Skala and Gilbert give a description of the latter in time, from formation to destruction.

In the reaction zone the rate of destruction of plastics based on organic resins can be determined over a broad temperature range from the relation

$$-\frac{dW_p}{d\tau} = B \exp(-E/RT) W_{vp} \left(\frac{W_p - W_c}{W_{vp}}\right)^n. \tag{19}$$

From (19) it follows that the weight of the plastic in the decomposition zone falls monotonically to the weight of the charred layer. As the temperature at the coke-reaction zone interface rises, the heat flow in the body and the rate of pyrolysis increase; as the temperature falls, they decrease, but the depth to which the heat shield is heated increases.

The total heat flow to the surface of the ablating material

$$q = q_{conv} + q_{comb} + q_{rad}. \tag{20}$$

The contribution q_{rad} is small and may often be neglected owing to the low emissivity of the gases.

Sometimes ablative materials are compared with respect to the effective heat of ablation

$$Q^* = q_0/\dot{m}. \tag{21}$$

It is assumed that the temperature and emissivity of the calorimeter are the same as at the surface of the charred layer of the heat shield.

It is important to know how the thickness of the charred layer varies with time. Skala and Gilbert found this relation by examining the pressure and temperature gradients over the section of the heat shield. The gas pressure drop in the internal pores of the charred layer creates mechanical stresses which may be expressed as

$$\sigma = P \frac{A_0}{A_s} - P_w \frac{A_w}{A_s}. \tag{22}$$

In addition, there are temperature stresses, and the two combined cause destruction of the charred layer and its removal from the region of maximum stress concentration, from the interface. The resulting curves respresenting the variation of the thickness of the charred layer with time and the temperature at its surface are saw-toothed. An increase in the ultimate tensile strength of the material causes an increase in the height of the "teeth" and the failure period.

Thus, in order to calculate the heat shield it is necessary to know the chemical reaction kinetics and the thermal and mechanical properties.

SUMMARY

To summarize, we may conclude that the various new high-temperature materials such as refractory metals and their alloys, metal borides, carbides, nitrides, and silicides, oxides, refractory coatings, and heat shields, can be studied by the methods of high-temperature thermophysics.

NOTATION

E is the potential difference across specimen, activation energy; I is the electric current through specimen; m, $\dot{m}$ are the mass of specimen and mass rate of ablation, respectively; t_0 is the temperature on the specimen axis; $dT/d\tau$ is the rate of change of temperature; Δt, Δt_l are the temperature drops along radius and axis of specimen, respectively; T, f (T) are the absolute temperature and heat removal from specimen surface, respectively; b is the parameter of the photoelectric pyrometer; ® is the reading of the

photoelectric pyrometer; c is the specific heat of the specimen; α is the temperature coefficient of resistance; R_0 is the electrical resistance at 0° C; R is the electrical resistance at mean temperature of specimen T_0, electrical resistance of working section, electrical resistance of phase shifter, and gas constant; G, A, AΔR are the weights of the specimen, heat value of calorimeter, and heat effect, respectively; $i_{0°C}^{t'_n}$ is the enthalpy from 0° C to t'_n (according to data of other authors); q_f, q_w, q_{s2} are the heat loss from the specimen on falling into the calorimeter, heat of tungsten suspension wires, and mean value of specific losses due to radiation at the cooler end, respectively; q, q_0, q_{conv}, q_{comb}, q_{rad} are the heat flow to the working section of the calorimeter and to nonablating surface of calorimeter and heat flows due to convection, chemical combustion reaction, and radiation, respectively; r, r_1, r_2 are the radius of specimen and distances from the axis of the specimen of points at which the temperature drop is measured, respectively; l is the working length of the calorimeter; ω is the oscillation frequency; C is the capacitance of the phase shifter; W_p, W_{vp}, W_c are the weights of plastic in pyrolysis zone, before pyrolysis and after pyrolysis, respectively; B is the effective collision frequency; n is the order of reaction; P, P_w are the local pressure in the charred layer and the pressure at the outer surface, respectively; A_0, A_s, A_w are the projections of the area of pores, the solid material, and the area of outer surface, respectively; $Q_{f.n}$ is the fast-neutron capture cross section in barns.

REFERENCES

1. V. A. Kirillin, Teplofizika vysokikh temperatur, 1, no. 1, 1963.

2. Industrial Heating, 28, 137, 1961.

3. Materials in Design Engineering, 53, 12, 1961.

4. V. A. Kirillin, A. E. Sheindlin, V. Ya. Chekhovskoi, and V. I. Tyukaev, Teplofizika vysokikh temperatur, 2, no. 4, 1964.

5. L. Prus et al., Nuclear Sci. and Engng., 6, 167, 1959.

6. S. Sindeband and P. Schwarzkopf, Powd. Met. Bull., 5, 42, 1950.

7. A. N. Krestovnikov and M. S. Bendrikh, Izv. VUZ. Tsvetnaya metallurgiya, no. 1, 1958.

8. P. Schwarzkopf and S. Sindeband, Vortrag Electrochem. Soc. Cleveland, 1950.

9. Taylor, J. Amer. Ceram. Soc., 44, no. 10, 1961.

10. B. Naylor, J. Amer. Chem. Soc., 68, 370, 1946.

11. R. Kieffer and F. Benesovsky, Werkstoffe für Raketentriebwerke. Acad. Verl.-Ges. Athenaion, Konstanz, 1961.

12. L. F. Mal'tseva and E. N. Marmer, Elektrotermiya, no. 31, 1964.

13. P. F. Gel'd and F. G. Kusenko, Izv. AN SSSR, OTN, Metallurgiya i toplivo, no. 2, 1960.

14. O. Kubaschevsky and E. Evans, Metallurgical Thermochemistry, London, 1951.

15. R. Kieffer and P. Schwarzkopf, Hard Alloys, 1957.

16. Financial Times, 1/I, 1958.

17. G. V. Samsonov and Ya. S. Umanskii, Hard Compounds of Refractory Metals [in Russian], 1957; G. V. Samsonov, Refractory Compounds [in Russian], 1963.

18. German Patent No. 437165, 1924.

19. T. Vasilos and W. Kingery, J. Amer. Ceram. Soc., 37, 409, 1954.

20. O. Kubaschevsky and E. Evans, Metallurgical Thermochemistry, London, 1951.

21. F. D. Frost, Metal Progress, 75, no. 3, 95, 1959; no. 4, 91, 1959.

22. H. H. Weigand, Stand der Entwicklung warmefester Titanlegierungen. WGL, Jahrbuch, 1959; Stahl Eisen, 80, 174, 301, 1960.

23. W. S. Pollini and W. Harris, Metal Progress, 77, no. 3, 69; no. 4, 113; no. 5, 83, 1960.

24. Preview of Space Metals, Metal Progress, 74, 96, 1958.

25. H. D. Nienhaus, Flugkörper, 2, no. 5, 143, 1960.

26. Kraus, Voprosy raketnoi tekhniki, no. 10, 1964.

27. Voprosy raketnoi tekhniki, no. 1, 41, 1966; no. 2, 34, 1966.

28. N. S. Rasor and J. D. McClelland, Rev. Sci. Instr., 31, no. 6, 595, 1960.

29. Ya. A. Kraftmakher, PMTF, no. 5, 1962.

30. V. A. Kirillin, A. E. Sheindlin, V. Ya. Chekhovskoi, DAN SSSR, 135, no. 1, 1960.

31. V. A. Kirillin, A. E. Sheindlin, V. Ya. Chekhovskoi, IFZh, 4, no. 2, 1961.

32. V. Ya. Chekhovskoi, candidate's dissertation, Moscow Power Engineering Institute, 1958.

33. V. A. Kirillin, A. E. Sheindlin, V. Ya. Chekhovskoi, and V. A. Petrov, ZhFKh, 37, no. 10, 1963.

34. V. Ya. Chekhovskoi and A. E. Sheindlin, PTE, no. 1, 1963.

35. D. L. Timrot and V. E. Peletskii, Teplofizika vysokikh temperatur, 1, no. 2, 1963.

36. V. Yu. Voskresenskii, author's abstract of dissertation, Moscow Power Engineering Institute, 1965.

37. O. A. Kraev, Teploenergetika, no. 4, 1956; no. 12, 1957; no. 4, 1958.

38. L. A. Brovkin, Zav. lab., no. 8, 1957; no. 5, 1961; Izv. VUZ. Energetika, no. 6, 1958; no. 7, 1959.

39. N. Yu. Taits and E. M. Gol'farb, Zav. lab., no. 4, 1959.

40. V. A. Osipova, Experimental Investigation of Heat Transfer Processes [in Russian], 1964.

41. O. A. Kraev and A. A. Stel'makh, Teplofizika vysokikh temperatur, 1, no. 1, 1963.

42. S. M. Skala and L. M. Gilbert, A. R. S. J., 32, 917, 1962.

3 June 1966

Institute of Heat and Mass Transfer AS BSSR, Minsk